Short-baseline neutrino oscillations and neutrinoless double-beta decay in the framework of three neutrino mixing and a mass hierarchy

S.M. Bilenky[a], A. Bottino[b], C. Giunti[b] and C. W. Kim[c]

[a]*Joint Institute for Nuclear Research, Dubna, Russia, and*

SISSA-ISAS, Trieste, Italy.

[b]*INFN, Sezione di Torino and Dipartimento di Fisica Teorica, Università di Torino,*

Via P. Giuria 1, 10125 Torino, Italy.

[c]*Department of Physics and Astronomy, The Johns Hopkins University,*

Baltimore, Maryland 21218, USA.

(February 2, 1996)

Abstract

We have analyzed the results of the latest terrestrial neutrino oscillation experiments in the framework of a model with mixing of three massive neutrinos and a neutrino mass hierarchy ($m_1 \ll m_2 \ll m_3$). In this model, oscillations of the terrestrial neutrinos are characterized by three parameters, $\Delta m^2 \equiv m_3^2 - m_1^2$ and the squared moduli of the two mixing matrix elements U_{e3} and $U_{\mu 3}$. Using the results of disappearance experiments and solar neutrino experiments, it is shown that only two regions of possible values of $|U_{e3}|^2$ and $|U_{\mu 3}|^2$ are allowed: I. $|U_{e3}|^2$ and $|U_{\mu 3}|^2$ are both small and II. $|U_{e3}|^2$ is small and $|U_{\mu 3}|^2$ is large. If the mixing parameters are in the region I, $\nu_\mu \leftrightarrows \nu_e$ oscillations are suppressed. In this case the LSND indication in favor of $\nu_\mu \leftrightarrows \nu_e$ oscillations is not compatible with the negative results of all other experiments. If the mixing parameters are in the region II, $\nu_e \leftrightarrows \nu_\tau$ oscillations are strongly suppressed. If massive neutrinos are Majorana particles, our analysis shows that neutrinoless double-beta decay could be observed in the experiments of the next generation only if the mixing parameters are in the region I.

Typeset using REVTEX

I. INTRODUCTION

The problem of neutrino masses and mixing is the most important problem in neutrino physics today. The search for the effects of neutrino masses and mixing is generally considered as one of the important and fertile ways to probe new scales in physics. As is well known, neutrino masses and mixing naturally arise in GUT models. The see-saw mechanism [1] of Majorana neutrino mass generation, that is characteristic of GUT models, is the only known mechanism that allows one to explain in a natural way the smallness of neutrino masses with respect to the masses of all the other fundamental fermions.

At present, there are several indications in favor of neutrino masses and mixing. It is a general opinion (see, for example, Ref. [2]) that the most convincing indications in favor of a small neutrino mass difference ($\Delta m^2 \simeq 10^{-5} \, \mathrm{eV}^2$) and neutrino mixing come from the results of the solar neutrino experiments. In all four solar neutrino experiments (Homestake, Kamiokande, GALLEX and SAGE) [3] the observed event rate is significantly lower than the event rate predicted by the Standard Solar Model (see Refs. [4–6]). A phenomenological analysis of the data that does not depend on the predictions of the Standard Solar Model indicates that the data of the different experiments are not compatible with each other if there are no transitions of solar ν_e's into other states [7].

In a recent experiment [8], the LSND collaboration found a positive indication in favor of $\bar{\nu}_\mu \to \bar{\nu}_e$ oscillations (see, however, also Ref. [9]). The LSND collaboration reported the detection of nine $\bar{\nu}_e p \to e^+ n$ events at a distance of about 30 m from a target in which neutrinos are produced in the decays of stopped π^+'s and μ^+'s. The LSND collaboration calculated [8] a background of 2.1 ± 0.3 events. As shown in Ref. [8], there is a region in the plane of the parameters Δm^2 and $\sin^2 2\theta$ (θ is the mixing angle) in which the LSND result is compatible with the exclusion plots obtained in other experiments [10,11] searching for $\nu_\mu \to \nu_e$ transitions.

In this paper we present an analysis of the results of the latest disappearance and appearance terrestrial neutrino oscillation experiments in the framework of a general scheme in which flavor neutrino fields are mixtures of three neutrino fields with masses that satisfy a hierarchy relation. In this scheme the oscillations among all active neutrinos ($\nu_\mu \leftrightarrows \nu_e$, $\nu_\mu \leftrightarrows \nu_\tau$, $\nu_e \leftrightarrows \nu_\tau$) are rather strongly constrained. We will show that, in the region of the values of the mixing parameters that is allowed by the results of reactor and accelerator disappearance experiments, the positive LSND result is not compatible with the negative results of all other experiments if there is a hierarchy of couplings in the lepton sector.

From the results of LEP experiments which measured the invisible width of the Z boson (see Ref. [12]) it follows that only three flavor neutrinos exist in nature. However, LEP data do not provide a constraint on the number of massive light neutrinos. The number of massive neutrinos depends on the neutrino mixing scheme. If the total lepton number is conserved, neutrinos are Dirac particles and the number of massive neutrinos is equal to the number of neutrino flavors. If the total lepton number is not conserved and only left-handed neutrino fields enter in the total Lagrangian (Majorana mass term), neutrinos with definite mass are Majorana particles and the number of massive neutrinos is again equal to the number of neutrino flavors. In the most general case of neutrino mixing, left-handed and right-handed flavor neutrino fields enter in the mass term and the total lepton number is not conserved (Dirac and Majorana mass term). In this case massive neutrinos are Majorana

particles and the number of particles with definite mass is twice the number of neutrino flavors. In the case of Dirac and Majorana mass term there is a very attractive mechanism which explains the smallness of the masses of light neutrinos, i.e. the see-saw mechanism [1]. If one assumes that the total lepton number is violated at the GUT scale M_{GUT} by a right-handed Majorana mass term and the parameters that characterize the Dirac mass term are of the order of the corresponding lepton or quark masses, then in the spectrum of Majorana particles there are three very heavy Majorana particles with masses $M_i \simeq M_{\mathrm{GUT}}$ and three light neutrinos with masses $m_k \simeq m_{\mathrm{Fk}}^2/M_{\mathrm{GUT}}$ (here $k = 1, 2, 3$ and m_{Fk} is the mass of the up-quark or charged lepton in the kth generation). In the see-saw scheme it is expected that the fields of flavor neutrinos are predominantly mixtures of the fields of the three light Majorana neutrinos. Thus, from a general theory of neutrino mixing it follows that the possibility of three massive neutrinos corresponding to the three existing flavor neutrinos is quite plausible.

It is to be noted that, if the number of massive neutrinos is more than three, oscillations between active and sterile neutrinos (neutrinos that do not take part in the standard weak interactions) are possible (see, for example, Ref. [13,14]). Future solar neutrino experiments (SNO [15], Super-Kamiokande [16]) could allow to check in a model independent way [17] if solar ^{8}B ν_e's transform into sterile states. Some possible scenarios with mixing of more than three massive neutrinos were considered in Ref. [18].

In this paper we will assume that three flavor neutrino fields $\nu_{\alpha L}$ (with $\alpha = e, \mu, \tau$) are given by a superposition of three (Dirac or Majorana) fields ν_{kL} with mass m_k as

$$\nu_{\alpha L} = \sum_{k=1}^{3} U_{\alpha k} \nu_{kL} \ . \tag{1.1}$$

Here U is a unitary mixing matrix.

The masses of all the known fundamental fermions (leptons and quarks) satisfy hierarchy relations. It is natural to assume that neutrino masses also satisfy the following hierarchy

$$m_1 \ll m_2 \ll m_3 \ . \tag{1.2}$$

If neutrino masses are generated with the see-saw mechanism, the hierarchy relation (1.2) is a consequence of the hierarchy of the lepton or quark masses.

We will consider oscillations of terrestrial neutrinos under the assumption that the squared mass difference $\Delta m_{21}^2 \equiv m_2^2 - m_1^2$ is small and can be relevant for an explanation of the deficit of solar ν_e's observed by all solar neutrino experiments [3] (say $\Delta m_{21}^2 \simeq 10^{-5}\,\mathrm{eV}^2$ as suggested by the MSW explanation of the solar neutrino problem [19,20]). Thus, for all experiments with terrestrial neutrinos we have $\Delta m_{21}^2 L/2p \ll 1$, where L is the distance between the neutrino source and detector, and p is the neutrino momentum.

Under these assumptions the amplitude of $\nu_\alpha \to \nu_\beta$ transitions can be written in the following form

$$\mathcal{A}_{\nu_\alpha \to \nu_\beta} = \mathrm{e}^{-\rangle \mathcal{E}_\infty \mathcal{L}} \left\{ \sum_{\|=\infty,\in} \mathcal{U}_{\beta\|} \mathcal{U}_{\alpha\|}^* + \mathcal{U}_{\beta\ni} \mathcal{U}_{\alpha\ni}^* \exp\left(-\rangle \frac{\cdot \Updownarrow^\in \mathcal{L}}{\in \sqrt{}} \right) \right\} , \tag{1.3}$$

3

with $\Delta m^2 \equiv m_3^2 - m_1^2$ and $E_k = \sqrt{p^2 + m_k^2} \simeq p + \dfrac{m_k^2}{2p}$. Then, taking into account the fact that, due to the unitarity of the mixing matrix,

$$\sum_{k=1,2} U_{\beta k} U_{\alpha k}^* = \delta_{\alpha\beta} - U_{\beta 3} U_{\alpha 3}^* \,, \tag{1.4}$$

for the probability of $\nu_\alpha \to \nu_\beta$ transitions with $\beta \neq \alpha$ we obtain the following expression (see, for example, Ref. [21])

$$P_{\nu_\alpha \to \nu_\beta} = \frac{1}{2} A_{\nu_\alpha;\nu_\beta} \left(1 - \cos \frac{\Delta m^2 L}{2\,p} \right) \,, \tag{1.5}$$

where

$$A_{\nu_\alpha;\nu_\beta} = A_{\nu_\beta;\nu_\alpha} = 4 \, |U_{\alpha 3}|^2 \, |U_{\beta 3}|^2 \tag{1.6}$$

is the amplitude of $\nu_\alpha \leftrightarrows \nu_\beta$ oscillations.

The expression for the probability of ν_α to survive can be derived from Eq.(1.5) and the conservation of the total probability as

$$P_{\nu_\alpha \to \nu_\alpha} = 1 - \sum_{\beta \neq \alpha} P_{\nu_\alpha \to \nu_\beta} = 1 - \frac{1}{2} B_{\nu_\alpha;\nu_\alpha} \left(1 - \cos \frac{\Delta m^2 L}{2\,p} \right) \,, \tag{1.7}$$

where the oscillation amplitude $B_{\nu_\alpha;\nu_\alpha}$ is given by

$$B_{\nu_\alpha;\nu_\alpha} = \sum_{\beta \neq \alpha} A_{\nu_\alpha;\nu_\beta} \,. \tag{1.8}$$

Using the unitarity of the mixing matrix, from Eqs.(1.6) and (1.8) we obtain

$$B_{\nu_\alpha;\nu_\alpha} = 4 \, |U_{\alpha 3}|^2 \left(1 - |U_{\alpha 3}|^2 \right) \,. \tag{1.9}$$

We wish to emphasize the following important features of terrestrial neutrino oscillations in the model under consideration.

1. All oscillation channels ($\nu_\mu \leftrightarrows \nu_e$, $\nu_\mu \leftrightarrows \nu_\tau$, $\nu_e \leftrightarrows \nu_\tau$) are open and the transition probabilities are determined by three parameters, Δm^2, $|U_{e3}|^2$ and $|U_{\mu 3}|^2$ (from the unitarity of the mixing matrix it follows that $|U_{\tau 3}|^2 = 1 - |U_{e3}|^2 - |U_{\mu 3}|^2$).

2. The oscillations in all channels are characterized by the *same* oscillation length $L_{\mathrm{osc}} = 4\pi p / \Delta m^2$ and the amplitudes of the inclusive transitions $\nu_\alpha \to \nu_\alpha$ and exclusive transitions $\nu_\alpha \to \nu_\beta$ ($\alpha \neq \beta$) are related by the relation (1.8).

3. The probabilities of $\nu_\alpha \to \nu_\beta$ and $\bar{\nu}_\alpha \to \bar{\nu}_\beta$ are equal, i.e.

$$P_{\nu_\alpha \to \nu_\beta} = P_{\bar{\nu}_\alpha \to \bar{\nu}_\beta} \,. \tag{1.10}$$

This relation is a consequence of the fact that the oscillation probabilities depend only on the squared moduli of the elements of the mixing matrix. In a general case of mixing of three massive neutrinos, Eq.(1.10) for $\alpha \neq \beta$ is satisfied only if CP is conserved in the lepton sector. Notice that Eq.(1.10) for $\alpha = \beta$ is a consequence of CPT invariance.

4

The expressions (1.5) and (1.7) have the same form as the standard expressions for the transition probabilities in the case of mixing between two massive neutrino fields. In the latter case only oscillations between two flavors are possible and the oscillation probabilities are characterized by two parameters, Δm^2 and $\sin^2 2\theta$. The important difference between the two-neutrino mixing scheme and the scheme with three-neutrino mixing and a mass hierarchy that we consider in the present paper is that the second scheme allows simultaneous transitions among all three flavor neutrinos. Some preliminary results of the analysis of the terrestrial neutrino oscillation experiments in the framework of this scheme were already presented in Ref. [22] and in this paper we wish to elaborate the details and present further new results.

II. ANALYSIS OF THE RESULTS OF NEUTRINO OSCILLATION EXPERIMENTS

We will present here an analysis of the results of the latest oscillation experiments with terrestrial neutrinos in the framework of the model with mixing of three massive neutrinos and a neutrino mass hierarchy. We will also consider the results of the LSND experiment, in which positive indications in favor of $\bar{\nu}_\mu \leftrightarrows \bar{\nu}_e$ oscillations were found [8]. The new experiments CHORUS [23] and NOMAD [24] searching for $\nu_\mu \to \nu_\tau$ transitions are under way at CERN. These experiments are sensitive to Δm^2 in a few eV^2 range (which is of great interest for the problem of dark matter in the universe) and to small values of the oscillation amplitude ($A_{\nu_\mu;\nu_\tau} \gtrsim 10^{-4}$). We will discuss possible implications of the results of these experiments for $\nu_\mu \leftrightarrows \nu_e$ oscillations after the projected sensitivity will be reached. We will also consider possible implications of the results of neutrino oscillation experiments for neutrinoless $\beta\beta$ decay ($(\beta\beta)_{0\nu}$) in the case of massive Majorana neutrinos.

A. Reactor and accelerator disappearance experiments

Let us start with the analysis of the results of reactor and accelerator disappearance experiments searching for $\nu_e \to \nu_x$ and $\nu_\mu \to \nu_x$ transitions. No indication in favor of neutrino oscillations was found in these experiments. We will use the exclusion plots obtained in the Bugey reactor experiment [25] and in the CDHS and CCFR84 accelerator experiments [26,27]. At fixed values of Δm^2, the allowed values of the amplitudes $B_{\nu_e;\nu_e}$ and $B_{\nu_\mu;\nu_\mu}$ are constrained by

$$B_{\nu_\alpha;\nu_\alpha} \leq B^0_{\nu_\alpha;\nu_\alpha} \qquad (\alpha = e, \mu) \ . \tag{2.1}$$

The values of $B^0_{\nu_e;\nu_e}$ and $B^0_{\nu_\mu;\nu_\mu}$ can be obtained from the corresponding exclusion curves.

The parameters $|U_{\alpha3}|^2$ (with $\alpha = e, \mu$) are expressed in terms of the amplitudes $B_{\nu_\alpha;\nu_\alpha}$ as

$$|U_{\alpha3}|^2 = \frac{1}{2}\left(1 \pm \sqrt{1 - B_{\nu_\alpha;\nu_\alpha}}\right) \ . \tag{2.2}$$

It is obvious that, due to the symmetry of Eq.(1.9) with respect to the interchange $|U_{\alpha3}|^2 \leftrightarrows 1 - |U_{\alpha3}|^2$, two values of $|U_{\alpha3}|^2$ correspond to the same value of $B_{\nu_\alpha;\nu_\alpha}$. Thus, from the

negative results of reactor and accelerator disappearance experiments, one can infer that the parameters $|U_{\alpha3}|^2$ at fixed values of Δm^2 must satisfy one of the following inequalities

$$|U_{\alpha3}|^2 \leq a_\alpha^0 \qquad (2.3)$$

or

$$|U_{\alpha3}|^2 \geq 1 - a_\alpha^0 , \qquad (2.4)$$

with

$$a_\alpha^0 \equiv \frac{1}{2}\left(1 - \sqrt{1 - B_{\nu_\alpha;\nu_\alpha}^0}\right) . \qquad (2.5)$$

We will consider values of Δm^2 in the interval, $10^{-1}\,\mathrm{eV}^2 \leq \Delta m^2 \leq 10^3\,\mathrm{eV}^2$, that covers the range where positive indications in favor of $\nu_\mu \leftrightarrows \nu_e$ oscillations were reported by the LSND collaboration [8]. The values of the parameters a_e^0 and a_μ^0 in this interval of Δm^2, that were obtained from the exclusion plots of the Bugey experiment [25] and of the CDHS and CCFR84 experiments [26,27], respectively, are presented in Fig.1. It can be seen from Fig.1 that in the region of Δm^2 under consideration a_e^0 is always small and a_μ^0 is small for $\Delta m^2 \gtrsim 0.5\,\mathrm{eV}^2$.

From Eqs.(2.3) and (2.4) it follows that the parameters $|U_{\alpha3}|^2$ are either small or large (i.e. close to one). However, due to the unitarity of the mixing matrix the parameters $|U_{e3}|^2$ and $|U_{\mu3}|^2$ must satisfy the inequality $|U_{e3}|^2 + |U_{\mu3}|^2 \leq 1$ and consequently they cannot be both large. Thus, on the basis of an analysis of the results of only the reactor and accelerator disappearance experiments, we reach the conclusion that the values of the parameters $|U_{e3}|^2$ and $|U_{\mu3}|^2$ can lie in one of the following three regions:

I. The region of small $|U_{e3}|^2$ and $|U_{\mu3}|^2$.

II. The region of small $|U_{e3}|^2$ and large $|U_{\mu3}|^2$.

III. The region of large $|U_{e3}|^2$ and small $|U_{\mu3}|^2$.

It can be shown [22] that the region III is excluded by the results of solar neutrino experiments. In fact, in the model under consideration the survival probability of the solar ν_e's is given by [28]

$$P_{\nu_e \to \nu_e} = \left(1 - |U_{e3}|^2\right)^2 P_{\nu_e \to \nu_e}^{(1,2)} + |U_{e3}|^4 , \qquad (2.6)$$

where $P_{\nu_e \to \nu_e}^{(1,2)}$ is the survival probability due to the mixing between the first and the second generations. If the parameter $|U_{e3}|^2$ is large, from Eq.(2.6) in the region of Δm^2 under consideration we have $P_{\nu_e \to \nu_e} \geq 0.92$ for all values of the neutrino energy. This large lower bound of the ν_e survival probability is not compatible with the results of solar neutrino experiments [3].

In the following, we will consider, in detail, the region I and the region II. We will take into account the results of all the latest appearance experiments searching for neutrino oscillations.

B. The region of small $|U_{e3}|^2$ and $|U_{\mu 3}|^2$

In the region I, the parameters $|U_{e3}|^2$ and $|U_{\mu 3}|^2$ are small and bounded as

$$|U_{e3}|^2 \leq a_e^0 \quad \text{and} \quad |U_{\mu 3}|^2 \leq a_\mu^0 , \tag{2.7}$$

where the quantities a_e^0 and a_μ^0 are given by Eq.(2.5) and in the interval of Δm^2 under consideration, take the values as presented in Fig.1. The region I is of great theoretical interest. It is now well established that the non-diagonal elements of the CKM mixing matrix of quarks, V, are small and satisfy the hierarchy $|V_{13}| \ll |V_{23}| \ll |V_{12}|$. Is this feature common to the quark and lepton sectors? A hierarchy of couplings in the lepton sector similar to the one in the quark sector can be realized only if the values of the parameters $|U_{e3}|^2$ and $|U_{\mu 3}|^2$ lie in the region I.

If the values of the parameters $|U_{e3}|^2$ and $|U_{\mu 3}|^2$ are in the region I, we can expect that $\nu_\mu \leftrightarrows \nu_e$ oscillations are suppressed with respect to $\nu_\mu \leftrightarrows \nu_\tau$ and $\nu_e \leftrightarrows \nu_\tau$ oscillations. In fact, in the region I, the amplitude of $\nu_\mu \leftrightarrows \nu_e$ oscillations is given by a product of two small quantities $|U_{e3}|^2$ and $|U_{\mu 3}|^2$, whereas the amplitudes of $\nu_\mu \leftrightarrows \nu_\tau$ and $\nu_e \leftrightarrows \nu_\tau$ oscillations are linear in one of these two small quantities (see Eq.(1.6)).

Let us consider, in detail, $\nu_\mu \leftrightarrows \nu_e$ oscillations. From the results of reactor and accelerator disappearance experiments, we obtain the following upper bound for the oscillation amplitude

$$A_{\nu_\mu;\nu_e} \leq 4\, a_e^0\, a_\mu^0 . \tag{2.8}$$

In Fig.2, we have plotted the curve that represents this upper bound, which was obtained from the results of the Bugey [25], CDHS [26] and CCFR84 [27] experiments (the curve passing through the circles). In Fig.2 we have also plotted the exclusion curves obtained in the BNL E776 [10] (dash-dotted line) and KARMEN [11] (dash-dot-dotted line) experiments searching for $\nu_\mu \rightarrow \nu_e$ transitions. The region allowed by the results of the LSND experiment is shown in Fig.2 as the shadowed region between the two solid lines. Taking into account that $A_{\nu_\mu;\nu_e} \leq B_{\nu_e;\nu_e}$ (see Eq.(1.8)), we have also plotted, in Fig.2, the exclusion curve for $B_{\nu_e;\nu_e}$ found in the Bugey experiment (dashed line). It can be seen from the figure that for small values of Δm^2 ($\Delta m^2 \lesssim 0.5\,\mathrm{eV}^2$) this bound on $A_{\nu_\mu;\nu_e}$ is stronger than the direct bound obtained by the BNL E776 and KARMEN experiments. It is also seen from the figure that this bound is not compatible with the result of the LSND experiment for $\Delta m^2 \lesssim 0.2\,\mathrm{eV}^2$.

Fig.2 shows that, in the range of Δm^2 under consideration, with the exception of the interval $10\,\mathrm{eV}^2 \lesssim \Delta m^2 \lesssim 60\,\mathrm{eV}^2$, the limits on the oscillation amplitude $A_{\nu_\mu;\nu_e}$ that can be obtained from the results of disappearance experiments are more stringent than the limits obtained from the experiments searching for $\nu_\mu \rightarrow \nu_e$ transitions. From Fig.2, it can be seen that the LSND result is not compatible with the results of the reactor and accelerator disappearance experiments in the range of Δm^2 under consideration, with the exception of the interval $5\,\mathrm{eV}^2 \lesssim \Delta m^2 \lesssim 70\,\mathrm{eV}^2$. In this interval of Δm^2 the result of the LSND experiment is only marginally compatible with the exclusion curve obtained in the BNL E776 experiment.

Thus, from the results of disappearance experiments we have obtained rather strong limits on the allowed values of the oscillation amplitude $A_{\nu_\mu;\nu_e}$ in the region I of the parameters $|U_{e3}|^2$ and $|U_{\mu 3}|^2$. We will take now into account also the results of the FNAL E531

experiment [29] on the search for $\nu_\mu \to \nu_\tau$ and $\nu_e \to \nu_\tau$ transitions and the recent results of the CCFR95 experiment [30] on the search for $\nu_\mu \to \nu_\tau$ transitions. From the exclusion plots deduced from these two experiments, for a fixed value of Δm^2, the values of $A_{\nu_\mu;\nu_\tau}$ and $A_{\nu_e;\nu_\tau}$ are constrained by

$$A_{\nu_\mu;\nu_\tau} \leq A^0_{\nu_\mu;\nu_\tau} \, , \tag{2.9}$$

$$A_{\nu_e;\nu_\tau} \leq A^0_{\nu_e;\nu_\tau} \, . \tag{2.10}$$

From Eq.(1.6) it follows that in the linear approximation in the small quantities $|U_{e3}|^2$ and $|U_{\mu3}|^2$ we have

$$|U_{\mu3}|^2 \simeq \frac{1}{4} A_{\nu_\mu;\nu_\tau} \, , \tag{2.11}$$

$$|U_{e3}|^2 \simeq \frac{1}{4} A_{\nu_e;\nu_\tau} \, . \tag{2.12}$$

Thus, the parameters $|U_{\mu3}|^2$ and $|U_{e3}|^2$ are determined, respectively, by the amplitudes of $\nu_\mu \leftrightarrows \nu_\tau$ and $\nu_e \leftrightarrows \nu_\tau$ oscillations. With the help of Eq.(2.11), from the results of the FNAL E531 and CCFR95 experiments it is possible to obtain, for $\Delta m^2 \gtrsim 4\,\text{eV}^2$, more stringent limits on the value of $|U_{\mu3}|^2$ than those obtained from the results of the CDHS and CCFR84 disappearance experiments. Combining these limits with the limits on $|U_{e3}|^2$ obtained from the results of the Bugey disappearance experiment, we have found rather stringent limits on the value of the amplitude $A_{\nu_\mu;\nu_e}$. In fact, from Eqs.(2.7) and (2.11) we have

$$A_{\nu_\mu;\nu_e} \lesssim a^0_e A^0_{\nu_\mu;\nu_\tau} \, . \tag{2.13}$$

The bound (2.13) on the amplitude $A_{\nu_\mu;\nu_e}$ obtained from the results of the Bugey, FNAL E531 and CCFR95 experiments is presented in Fig.2 (the curve passing through the triangles). It can be seen in Fig.2 that the results of reactor and accelerator disappearance experiments, together with the results of $\nu_\mu \to \nu_\tau$ appearance experiments exclude all the region of the parameters Δm^2 and $A_{\nu_\mu;\nu_e}$ that is allowed by the LSND experiment. It is to be emphasized that this result has been derived under the assumption that the parameters $|U_{e3}|^2$ and $|U_{\mu3}|^2$ are both small.

In Fig.2, we have also shown the region in the $A_{\nu_\mu;\nu_e}$–Δm^2 plane that could be explored when the projected sensitivity of the CHORUS [23] and NOMAD [24] experiments, which are searching for $\nu_\mu \to \nu_\tau$ transitions, is reached (the region delimited by the line passing through the squares).

From Eqs.(2.11) and (2.12) we obtain the following inequality

$$A_{\nu_\mu;\nu_e} \lesssim \frac{1}{4} A^0_{\nu_\mu;\nu_\tau} A^0_{\nu_e;\nu_\tau} \, . \tag{2.14}$$

The limits obtained, by using this inequality, from the results of the FNAL E531 and CCFR95 experiments on the search for $\nu_\mu \to \nu_\tau$ transitions and from the results of the FNAL E531 experiment on the search for $\nu_e \to \nu_\tau$ transitions are presented in Fig.2 (the dotted line).

Finally, since in the region I the amplitude $A_{\nu_\mu;\nu_e}$ is very small, we obtain, from Eq.(1.8), the following relations between the amplitudes of inclusive and exclusive transitions

$$B_{\nu_\mu;\nu_\mu} \simeq A_{\nu_\mu;\nu_\tau} , \qquad (2.15)$$

$$B_{\nu_e;\nu_e} \simeq A_{\nu_e;\nu_\tau} . \qquad (2.16)$$

A test of these relations will allow us to check if there is a hierarchy of masses and couplings in the lepton sector.

C. The region of small $|U_{e3}|^2$ and large $|U_{\mu3}|^2$

We will now consider in detail the region II in which the parameter $|U_{e3}|^2$ is small and $|U_{\mu3}|^2$ is large (close to one), i.e.

$$|U_{e3}|^2 \leq a_e^0 \quad \text{and} \quad |U_{\mu3}|^2 \geq 1 - a_\mu^0 , \qquad (2.17)$$

with the quantities a_e^0 and a_μ^0 given by Eq.(2.5).

In this region, $\nu_e \leftrightarrows \nu_\tau$ oscillations are strongly suppressed with respect to $\nu_\mu \leftrightarrows \nu_e$ and $\nu_\mu \leftrightarrows \nu_\tau$ oscillations. This is due to the fact that the amplitude $A_{\nu_e;\nu_\tau}$ is quadratic in the small quantities $|U_{e3}|^2$ and $(1 - |U_{\mu3}|^2)$, whereas the amplitudes $A_{\nu_\mu;\nu_e}$ and $A_{\nu_\mu;\nu_\tau}$ are linear (see Eq.(1.6)).

Taking into account the unitarity bound $|U_{e3}|^2 \leq 1 - |U_{\mu3}|^2$, it follows from Eq.(2.17) that the parameter $|U_{e3}|^2$ must also satisfy the following inequality

$$|U_{e3}|^2 \leq a_\mu^0 . \qquad (2.18)$$

From Eqs.(2.17) and (2.18), we obtain the following upper bound for the amplitude of $\nu_e \leftrightarrows \nu_\tau$ oscillations

$$A_{\nu_e;\nu_\tau} \leq 4 \, \text{Min} \left[a_e^0, a_\mu^0 \right] a_\mu^0 . \qquad (2.19)$$

From this inequality it follows that $\nu_e \leftrightarrows \nu_\tau$ oscillations are strongly suppressed in the region II. In Fig.3, we have plotted the upper bound for the amplitude $A_{\nu_e;\nu_\tau}$ obtained from Eq.(2.19) using the results of the Bugey, CDHS and CCFR84 experiments (the curve passing through the triangles). From this figure it can be seen that in all the considered range of Δm^2 the upper bound for $A_{\nu_e;\nu_\tau}$ is very small, varying from about 10^{-4} to about 4×10^{-2}.

Up to now we have used the limits on the parameters $|U_{e3}|^2$ and $|U_{\mu3}|^2$ that were obtained from the results of disappearance experiments. We will now take into account also the results of the BNL E776 experiment [10] that has searched for $\nu_\mu \to \nu_e$ transitions. From the exclusion plot obtained in this experiment, it follows that, for a fixed value of Δm^2, the value of the $\nu_\mu \leftrightarrows \nu_e$ oscillation amplitude is constrained by

$$A_{\nu_\mu;\nu_e} \leq A_{\nu_\mu;\nu_e}^0 . \qquad (2.20)$$

Since in the region II under consideration, the parameter $|U_{\mu3}|^2$ is close to one in the linear approximation in the small quantities $|U_{e3}|^2$ and $\left(1 - |U_{\mu3}|^2\right)$, we have

$$A_{\nu_\mu;\nu_e} \simeq 4 \, |U_{e3}|^2 \; . \tag{2.21}$$

From this relation and Eq.(2.20) we have

$$|U_{e3}|^2 \lesssim \frac{A^0_{\nu_\mu;\nu_e}}{4} \; . \tag{2.22}$$

The upper bound for $|U_{e3}|^2$ obtained from the results of the BNL E776 experiment are presented in Fig.4 (the dashed curve). From this figure it can be seen that for $0.7\,\mathrm{eV}^2 \lesssim \Delta\mathrm{m}^2 \lesssim 10^3\,\mathrm{eV}^2$ the limits on the parameter $|U_{e3}|^2$ that can be found from the results of the BNL E776 experiment are much more stringent than those obtained from the exclusion plot of the Bugey experiment (dash-dotted curve) and from the results of the CDHS and CCFR experiments with Eq.(2.18) (dash-dot-dotted curve).

From the positive results of the LSND experiment, we can find a region of *allowed* values of $|U_{e3}|^2$ in the $|U_{e3}|^2$–Δm^2 plane. In fact, for a fixed value of Δm^2, from the LSND allowed region in the $A_{\nu_\mu;\nu_e}$–Δm^2 plane, we have

$$A^{(-)}_{\nu_\mu;\nu_e} \leq A_{\nu_\mu;\nu_e} \leq A^{(+)}_{\nu_\mu;\nu_e} \; . \tag{2.23}$$

Hence, with Eq.(2.21) we obtain

$$\frac{A^{(-)}_{\nu_\mu;\nu_e}}{4} \lesssim |U_{e3}|^2 \lesssim \frac{A^{(+)}_{\nu_\mu;\nu_e}}{4} \; . \tag{2.24}$$

The corresponding allowed region is presented in Fig.4 (the shadowed region between the solid lines).

From the inequality (2.22), it is possible to derive the following upper bound for the amplitude of $\nu_e \leftrightarrows \nu_\tau$ oscillations

$$A_{\nu_e;\nu_\tau} \lesssim A^0_{\nu_\mu;\nu_e} \, a^0_\mu \; . \tag{2.25}$$

In Fig.3 we have plotted the corresponding boundary curve obtained from the results of the CDHS, CCFR84 and BNL E776 experiments (the curve passing through the squares). From this figure it can be seen that for $\Delta m^2 \gtrsim 1\,\mathrm{eV}^2$ the upper bound on the oscillation amplitude $A_{\nu_e;\nu_\tau}$ varies from 2×10^{-5} to 5×10^{-4} and is more stringent than that obtained from the results of disappearance experiments using Eq.(2.19).

From the results of the experiments searching for $\nu_\mu \rightarrow \nu_\tau$ transitions, we can obtain even stronger limits on the amplitude of $\nu_e \leftrightarrows \nu_\tau$ oscillations. In fact, in the region II under consideration, where $|U_{\mu3}|^2 \simeq 1$, the negative results of the experiments searching for $\nu_\mu \rightarrow \nu_\tau$ transitions give the following upper bound on the value of $|U_{\tau3}|^2$

$$|U_{\tau3}|^2 \lesssim \frac{A^0_{\nu_\mu;\nu_\tau}}{4} \; . \tag{2.26}$$

From Eqs.(2.22) and (2.26) we have the following constraint on the amplitude of $\nu_e \leftrightarrows \nu_\tau$ oscillations

10

$$A_{\nu_e;\nu_\tau} \lesssim \frac{A^0_{\nu_\mu;\nu_e} A^0_{\nu_\mu;\nu_\tau}}{4} \; . \tag{2.27}$$

The corresponding boundary curve obtained from the results of the BNL E776, FNAL E531 and CCFR95 experiments is presented in Fig.3 (the curve passing through the circles). From this figure it can be seen that for $\Delta m^2 \gtrsim 4\,\mathrm{eV}^2$ the amplitude of $\nu_e \leftrightarrows \nu_\tau$ oscillations is extremely small (less than 3×10^{-5}).

Furthermore, from Eqs.(2.22) and (2.26), we have

$$1 - |U_{\mu 3}|^2 \lesssim \frac{A^0_{\nu_\mu;\nu_e} + A^0_{\nu_\mu;\nu_\tau}}{4} \; . \tag{2.28}$$

The upper bound for $1 - |U_{\mu 3}|^2$ obtained with Eq.(2.28) from the results of the BNL E776, FNAL E531 and CCFR95 experiments is presented in Fig.5 (the dashed line). The solid line in Fig.5 represents the upper bound (2.17) obtained from the results of the CDHS and CCFR84 experiments. This figure shows that the inequality (2.28) enables us to obtain, in a wide range of values of Δm^2, more stringent limits on the values of the parameter $|U_{\mu 3}|^2$ from the results of the experiments on the search for $\nu_\mu \to \nu_e$ and $\nu_\mu \to \nu_\tau$ transitions than those obtained from the results of ν_μ disappearance experiments.

Finally, the fact that the amplitude $A_{\nu_e;\nu_\tau}$ is very small leads to the following relations between the amplitudes of inclusive $\nu_\alpha \to \nu_\alpha$ and exclusive $\nu_\alpha \to \nu_\beta$ ($\beta \neq \alpha$) transitions

$$B_{\nu_e;\nu_e} \simeq A_{\nu_\mu;\nu_e} \; , \tag{2.29}$$

$$B_{\nu_\mu;\nu_\mu} = A_{\nu_\mu;\nu_e} + A_{\nu_\mu;\nu_\tau} \; . \tag{2.30}$$

Thus, in the region II the amplitudes $B_{\nu_e;\nu_e}$ and $B_{\nu_\mu;\nu_\mu}$ are determined by the amplitudes $A_{\nu_\mu;\nu_e}$ and $A_{\nu_\mu;\nu_\tau}$. From the results of the LSND experiment and using Eqs.(2.9), (2.20), (2.23), (2.29) and (2.30), we obtain

$$A^{(-)}_{\nu_\mu;\nu_e} \lesssim B_{\nu_e;\nu_e} \lesssim \mathrm{Min}\left[A^{(+)}_{\nu_\mu;\nu_e}, A^0_{\nu_\mu;\nu_e} \right] \; , \tag{2.31}$$

$$A^{(-)}_{\nu_\mu;\nu_e} \leq B_{\nu_\mu;\nu_\mu} \leq \mathrm{Min}\left[A^{(+)}_{\nu_\mu;\nu_e}, A^0_{\nu_\mu;\nu_e} \right] + A^0_{\nu_\mu;\nu_\tau} \; . \tag{2.32}$$

A test of these relations in future reactor and accelerator experiments could allow us to check the indications in favor of $\nu_\mu \leftrightarrows \nu_e$ oscillations found by the LSND collaboration.

III. NEUTRINOLESS $\beta\beta$ DECAY

As we have shown in Section II A, in the framework of the model under consideration, the results of the solar neutrino experiments and those of the reactor and accelerator neutrino oscillation disappearance experiments indicate that the parameter $|U_{e3}|^2$ is small. If massive neutrinos are Majorana particles, this fact can have important consequences for $(\beta\beta)_{0\nu}$ decay experiments. The matrix element of $(\beta\beta)_{0\nu}$ decay is proportional to $\langle m \rangle = \sum_i U^2_{ei}\, m_i$ (see, for example, Refs. [13,14]). The results of the experiments searching for $(\beta\beta)_{0\nu}$ decay can be

summarized as $|\langle m \rangle| \lesssim 1\,\text{eV}$ (see Ref. [31]). The expected sensitivity of the next generation of experiments is $|\langle m \rangle| \simeq 10^{-1}\,\text{eV}$ [31].

In the framework of the model under consideration, the hierarchy of neutrino masses implies that [32]

$$|\langle m \rangle| \simeq |U_{e3}|^2 \sqrt{\Delta m^2} \,. \tag{3.1}$$

In Fig.6 we have plotted the boundary curve for $|\langle m \rangle|$ obtained with Eq.(3.1) from the results of the Bugey experiment in the interval $10^{-1}\,\text{eV}^2 \le \Delta m^2 \le 10^3\,\text{eV}^2$ (the dash-dotted line). From this figure it can be seen that for $\Delta m^2 \lesssim 5\,\text{eV}^2$, the upper bound for $|\langle m \rangle|$ is less than the projected sensitivity of the $(\beta\beta)_{0\nu}$ decay experiments of the next generation.

In the region II, where $|U_{e3}|^2$ is small and $|U_{\mu 3}|^2$ is large, the value of $|U_{e3}|^2$ is constrained not only by Eq.(2.17), but also by Eq.(2.18), which takes into account the unitarity constraint. In Fig.7 we have plotted the corresponding curve obtained from the results of the CDHS and CCFR84 experiments (the dash-dot-dotted line). Furthermore, in region II the value of $|U_{e3}|^2$ is severely constrained by the results of the BNL E776 experiment that searched for $\nu_\mu \to \nu_e$ transitions (see Eq.(2.22)). The corresponding boundary curve is presented in Fig.7 (the dashed curve). From this figure it can be seen that $|\langle m \rangle| \lesssim 10^{-2}\,\text{eV}$ practically in all the considered range of Δm^2. Thus, if the parameters $|U_{e3}|^2$ and $|U_{\mu 3}|^2$ are in the region II, the observation of $(\beta\beta)_{0\nu}$ decay becomes a formidable, if not impossible, task.

Finally, from the results of the LSND experiment, for each value of Δm^2, an allowed range of $|U_{e3}|^2$ can be determined from Eq.(2.24) in region II. In Fig.7 we have also plotted the corresponding allowed region in the Δm^2–$|\langle m \rangle|$ plane (the shadowed region between the two solid lines).

IV. CONCLUSIONS

We have considered a scheme with mixing of three massive neutrino fields and a hierarchy of neutrino masses. We have assumed that the squared mass difference $m_2^2 - m_1^2$ is small and can be relevant for the suppression of solar ν_e's. In this scheme the oscillations of terrestrial neutrinos in short-baseline experiments are determined by the values of three parameters, one squared mass difference $\Delta m^2 \equiv m_3^2 - m_1^2$ and the squared moduli of the two mixing matrix elements U_{e3} and $U_{\mu 3}$.

After the calibration of the GALLEX detector with a radioactive source [33] the indications in favor of neutrino oscillations coming from solar neutrino experiments have become more significant. For this reason, we believe that the model considered here is the simplest and most realistic model of neutrino mixing. It seems very appropriate to analyze in the framework of this model all the data from the existing experiments that have searched for neutrino oscillations and to infer predictions for the results of future experiments (see also Refs. [34,35]). In our discussion, we have also taken into account the positive indications in favor of $\nu_\mu \leftrightarrows \nu_e$ oscillations that were found in the recent LSND experiment.

We have shown, by using the results of reactor and accelerator disappearance experiments, that in a wide range of Δm^2 ($0.5\,\text{eV}^2 \le \Delta m^2 \le 10^3\,\text{eV}^2$) the parameters $|U_{e3}|^2$ and $|U_{\mu 3}|^2$ can be either very small or very large (close to 1). From the unitarity of the mixing

matrix and from the results of the solar neutrino experiments it follows that only two regions for the parameters $|U_{e3}|^2$ and $|U_{\mu 3}|^2$ are allowed:

I. The region of small $|U_{e3}|^2$ and $|U_{\mu 3}|^2$.

II. The region of small $|U_{e3}|^2$ and large $|U_{\mu 3}|^2$.

The overall situation for the allowed regions in the present theoretical framework is summarized in Figs.8 and 9. In these figures the various constraints and the allowed regions for the values of the parameters $|U_{e3}|^2$ and $|U_{\mu 3}|^2$ are displayed at the representative value $\Delta m^2 = 6\,\mathrm{eV}^2$.

If the parameters $|U_{e3}|^2$ and $|U_{\mu 3}|^2$ are in the region I, $\nu_\mu \leftrightarrows \nu_e$ oscillations are strongly suppressed. We have shown that in the region I the indications in favor of $\nu_\mu \leftrightarrows \nu_e$ oscillations found in the LSND experiment are not compatible with the results of all other experiments which have not found any evidence of neutrino oscillations. It is to be emphasized that a hierarchy of couplings in the lepton sector analogous to that of the quark sector is possible only if the parameters $|U_{e3}|^2$ and $|U_{\mu 3}|^2$ lie in region I.

If the parameters $|U_{e3}|^2$ and $|U_{\mu 3}|^2$ are in the region II, the amplitude of $\nu_e \leftrightarrows \nu_\tau$ oscillations is very small in the wide range of Δm^2 under consideration. In this case there is no constraint on the amplitudes of $\nu_\mu \leftrightarrows \nu_e$ and $\nu_\mu \leftrightarrows \nu_\tau$ oscillations and the amplitudes that characterize the survival probabilities of ν_e's and ν_μ's are determined by the amplitudes $A_{\nu_\mu;\nu_e}$ and $A_{\nu_\mu;\nu_\tau}$. The indication in favor of $\nu_\mu \leftrightarrows \nu_e$ oscillations found in the LSND experiment can be checked in future disappearance experiments.

We have also discussed the implications of our analysis for $(\beta\beta)_{0\nu}$ decay if massive neutrinos turn out to be Majorana particles. If the parameters $|U_{e3}|^2$ and $|U_{\mu 3}|^2$ lie in the region I and $\Delta m^2 \gtrsim 5\,\mathrm{eV}^2$, $(\beta\beta)_{0\nu}$ decay could be observed in the next generation of experiments. If the parameters $|U_{e3}|^2$ and $|U_{\mu 3}|^2$ are in the region II, the sensitivity of the $(\beta\beta)_{0\nu}$ decay experiments of the next generation is not sufficient to observe this process.

REFERENCES

[1] M. Gell-Mann, P. Ramond, and R. Slansky, in *Supergravity*, ed. F. van Nieuwenhuizen and D. Freedman, (North Holland, Amsterdam, 1979) p. 315; T. Yanagida, *Proc. of the Workshop on Unified Theory and the Baryon Number of the Universe*, KEK, Japan, 1979; S. Weinberg, Phys. Rev. Lett. **43**, 1566 (1979).

[2] K. Winter, preprint CERN-PPE/95-165, Invited Talk at the 17th International Symposium on Lepton-Photon Interactions, Beijing, China, 1995.

[3] B.T. Cleveland et al., Nucl. Phys. B (Proc. Suppl.) **38**, 47 (1995); K. S. Hirata et al., Phys. Rev. D **44**, 2241 (1991); GALLEX Coll., Phys. Lett. B **357**, 237 (1995); V.N. Gavrin, Talk presented at TAUP 95 Toledo (Spain), Sept. 1995.

[4] J.N. Bahcall and R. Ulrich, Rev. Mod. Phys. **60**, 297 (1988); J.N. Bahcall, *Neutrino Physics and Astrophysics*, Cambridge University Press, 1989; J.N. Bahcall and M.H. Pinsonneault, Rev. Mod. Phys. **64**, 885 (1992); IASSNS-AST-95-24 (hep-ph/9505425).

[5] S. Turck-Chièze, S. Cahen, M. Cassé and C. Doom, Astrophys. J. **335**, 415 (1988); S. Turck-Chièze and I. Lopes, Astrophys. J. **408**, 347 (1993); S. Turck-Chièze et al., Phys. Rep. **230**, 57 (1993).

[6] V. Castellani, S. Degl'Innocenti and G. Fiorentini, Astronomy & Astrophysics **271**, 601 (1993); S. Degl'Innocenti, Univ. of Ferrara preprint INFN-FE-07-93.

[7] V. Castellani et al., Astron. Astrophys. **271**, 601 (1993); S.A. Bludman et al., Phys. Rev. D **49**, 3622 (1994); V. Berezinsky, Comm. Nucl. Part. Phys. **21**, 249 (1994); J.N. Bahcall, Phys. Lett. B **338**, 276 (1994).

[8] C. Athanassopoulos et al., Phys. Rev. Lett. **75**, 2650 (1995).

[9] J.E. Hill, Phys. Rev. Lett. **75**, 2654 (1995).

[10] L. Borodovsky et al., Phys. Rev. Lett. **68**, 274 (1992).

[11] B. Armbruster et al., Nucl. Phys. B (Proc. Suppl.) **38**, 235 (1995).

[12] Review of Particle Properties, Phys. Rev. D **50**, 1173 (1994).

[13] S.M. Bilenky and B. Pontecorvo, Phys. Rep. **41**, 225 (1978); S.M. Bilenky and S.T. Petcov, Rev. Mod. Phys. **59**, 671 (1987).

[14] C.W. Kim and A. Pevsner, *Neutrinos in Physics and Astrophysics*, Contemporary Concepts in Physics, Vol. 8, (Harwood Academic Press, Chur, Switzerland, 1993).

[15] SNO Coll., Phys. Lett. B **194**, 321 (1987); H.H. Chen, Nucl. Instr. Meth. A **264**, 48 (1988).

[16] C.B. Bratton et al., *Proposal to Participate in the Super-Kamiokande Project*, Dec. 1992.

[17] S.M. Bilenky and C. Giunti, Z. Phys. C **68**, 495 (1995).

[18] D.O. Caldwell and R.N. Mohapatra, Phys. Rev. D **48**, 3259 (1993); J.T. Peltoniemi and J.W.F. Valle, Nucl. Phys. B **406**, 409 (1993); Z. Shi, D.N. Schramm and B.D. Fields, Phys. Rev. D **48**, 2563 (1993); J.R. Primack et al., Phys. Rev. Lett. **74**, 2160 (1995); G.M. Fuller, J.R. Primack and Y.Z. Qian, Phys. Rev. D **52**, 1288 (1995); G. Raffelt and J. Silk, hep-ph/9502306; E. Ma and P. Roy, Phys. Rev. D **52**, R4780 (1995).

[19] S.P. Mikheyev and A.Yu. Smirnov, Yad. Fiz. **42**, 1441 (1985) [Sov. J. Nucl. Phys. **42**, 913 (1985)]; Il Nuovo Cimento C **9**, 17 (1986); L. Wolfenstein, Phys. Rev. D **17**, 2369 (1978); Phys. Rev. D **20**, 2634 (1979).

[20] GALLEX Coll., Phys. Lett. B **285**, 390 (1992); X. Shi, D.N. Schramm and J.N. Bahcall, Phys. Rev. Lett. **69**, 717 (1992); S.A. Bludman, N. Hata, D.C. Kennedy and P.G.

Langacker, Phys. Rev. D **47**, 2220 (1993); N. Hata and P.G. Langacker, Phys. Rev. **50**, 632 (1994); P.I. Krastev and S.T. Petcov, Phys. Lett. B **299**, 99 (1993); Nucl. Phys. B **449**, 605 (1995); L.M. Krauss, E. Gates and M. White, Phys. Lett. B **299**, 94 (1993); Phys. Rev. D **51**, 2631 (1995); G.L. Fogli and E. Lisi, Astropart. Phys. **2**, 91 (1994); G. Fiorentini et al., Phys. Rev. D **49**, 6298 (1994).

[21] A. De Rujula et al., Nucl. Phys. B **168**, 54 (1980); V. Barger and K. Whisnant, Phys. Lett. B 209 (1988) 365; S.M. Bilenky, M. Fabbrichesi and S.T. Petcov, Phys. Lett. B **276**, 223 (1992).

[22] S.M. Bilenky, A. Bottino, C. Giunti and C.W. Kim, Phys. Lett. B **356**, 273 (1995).

[23] G. Rosa, Nucl. Phys. B (Proc.Suppl.) **40**, 85 (1995); D. Macina, Talk presented at TAUP 95 Toledo (Spain), Sept. 1995.

[24] A. Rubbia, Nucl. Phys. B (Proc.Suppl.) **40**, 93 (1995); M. Laveder, Talk presented at TAUP 95 Toledo (Spain), Sept. 1995 (hep-ph/9601342).

[25] B. Achkar et al., Nucl. Phys. B **434**, 503 (1995).

[26] F. Dydak et al., Phys. Lett. B **134**, 281 (1984).

[27] I.E. Stockdale et al., Phys. Rev. Lett. **52**, 1384 (1984).

[28] X. Shi and D.N. Schramm, Phys. Lett. B **283**, 305 (1992).

[29] N. Ushida Phys. Rev. Lett. **57**, 2897 (1986).

[30] K.S. McFarland et al., Phys. Rev. Lett. **75**, 3993 (1995).

[31] M.K. Moe, Nucl. Phys. B (Proc. Suppl.) **38**, 36 (1995).

[32] S.T. Petcov and A.Yu. Smirnov, Phys. Lett. B **322**, 109 (1994).

[33] GALLEX Coll., Phys. Lett. B **342**, 440 (1995).

[34] G.L. Fogli, E. Lisi and D. Montanino, Phys. Rev. D 49 (1994) 3626; Astropart. Phys. **4**, 177 (1995); G.L. Fogli, E. Lisi and G. Scioscia, Phys. Rev. D **52**, 5334 (1995).

[35] H. Minakata, Phys. Lett. B **356**, 61 (1995); Phys. Rev. D **52**, 6630 (1995).

FIGURES

FIG. 1. Values of the parameters a_e^0 and a_μ^0 (see Eq.(2.5)) obtained from the results of reactor and accelerator disappearance experiments for Δm^2 in the range $10^{-1}\,\mathrm{eV}^2 \leq \Delta\mathrm{m}^2 \leq 10^3\,\mathrm{eV}^2$.

FIG. 2. Exclusion regions in the $A_{\nu_\mu;\nu_e}$–Δm^2 plane for small $|U_{e3}|^2$ and $|U_{\mu3}|^2$. The regions excluded by the BNL E776 and KARMEN $\nu_\mu \leftrightarrows \nu_e$ appearance experiments are bounded by the dash-dotted and dash-dot-dotted curves, respectively. The dashed line represents the results of the Bugey experiment. The curve passing through the circles is obtained from the results of the Bugey, CDHS and CCFR84 experiments using Eq.(2.8). The curve passing through the triangles is obtained from the results of the Bugey, FNAL E531 and CCFR95 experiments using Eq.(2.13). The dotted line is obtained from the results of the FNAL E531 and CCFR95 experiments using Eq.(2.14). The line passing through the squares bounds the region that will be explored by CHORUS and NOMAD. The region allowed by the LSND experiment is also shown (the shadowed region limited by the two solid curves).

FIG. 3. Exclusion regions in the $A_{\nu_e;\nu_\tau}$–Δm^2 plane for small $|U_{e3}|^2$ and large $|U_{\mu3}|^2$. The solid line represents the results of the FNAL E531 experiment. The dashed line was obtained from the results of the Bugey experiment. The curve passing through the triangles is obtained from the results of the Bugey, CDHS and CCFR84 experiments using Eq.(2.19). The curve passing through the squares is obtained from the results of the CDHS, CCFR84 and BNL E776 experiments using Eq.(2.25). The curve passing through the circles is obtained from the results of the BNL E776, FNAL E531 and CCFR95 experiments using Eq.(2.27).

FIG. 4. Upper bounds for $|U_{e3}|^2$ in the region of small $|U_{e3}|^2$ and large $|U_{\mu3}|^2$. The dash-dotted and dash-dot-dotted curves are obtained from the results of the Bugey experiment and from the results of the CDHS and CCFR84 experiments, respectively (with the help of Eq.(2.18)). The dashed curve is obtained from the results of the BNL E776 experiment using Eq.(2.22). The shadowed region within the two solid lines is the allowed region obtained from the results of the LSND experiment using Eq.(2.24).

FIG. 5. Upper bounds for $1-|U_{\mu3}|^2$ in the region of small $|U_{e3}|^2$ and large $|U_{\mu3}|^2$. The solid curve was obtained from the results of the CDHS and CCFR95 experiments (see Eq.(2.17)). The dashed curve was obtained from the results of the BNL E776, FNAL E531 and CCFR95 experiments using Eq.(2.28).

FIG. 6. Boundary curve in the Δm^2–$|\langle m\rangle|$ plane for small $|U_{e3}|^2$ and $|U_{\mu3}|^2$. The curve was obtained from the results of the Bugey experiment.

FIG. 7. Boundary curves in the Δm^2–$|\langle m \rangle|$ plane for small $|U_{e3}|^2$ and large $|U_{\mu 3}|^2$. The dash-dotted and dash-dot-dotted curves are obtained from the results of the Bugey experiment and the results of the CDHS and CCFR84 experiments, respectively. The dashed curve is obtained from the results of the BNL E776 experiment. The shadowed region within the two solid lines is the allowed region obtained from the results of the LSND experiment.

FIG. 8. The regions I and II of the values of the parameters $|U_{e3}|^2$ and $|U_{\mu 3}|^2$ for $\Delta m^2 = 6 \, \text{eV}^2$. The vertical axis has been expanded logarithmically for $|U_{\mu 3}|^2$ very small and very large (i.e. close to one) using the two different coordinates, $|U_{\mu 3}|^2$ below the horizontal solid line and $(1 - |U_{\mu 3}|^2)$ above the horizontal solid line. We have drawn the constraints given by the results of the Bugey and CDHS disappearance experiments, which delimit the allowed regions I and II. The black region is excluded by unitarity.

FIG. 9. Allowed regions for the values of the parameters $|U_{e3}|^2$ and $|U_{\mu 3}|^2$ for $\Delta m^2 = 6 \, \text{eV}^2$. The vertical axis has been expanded logarithmically as in Fig.8. We have drawn the constraints given by the results of the Bugey and CDHS disappearance experiments (as in Fig.8) and the constraints given by the results of the BNL E776 ($\nu_\mu \to \nu_e$) and FNAL E531 ($\nu_\mu \to \nu_\tau$) experiments. The region allowed by the LSND experiment is shown as a lightly shadowed band. The darkly shadowed region is excluded by unitarity. The region Ia is the part of region I which is allowed by all experiments, except LSND. The region IIa is the part of region II which is allowed by all experiments, except LSND, whereas the region IIb is the part of region II which is allowed by all experiments, including LSND.
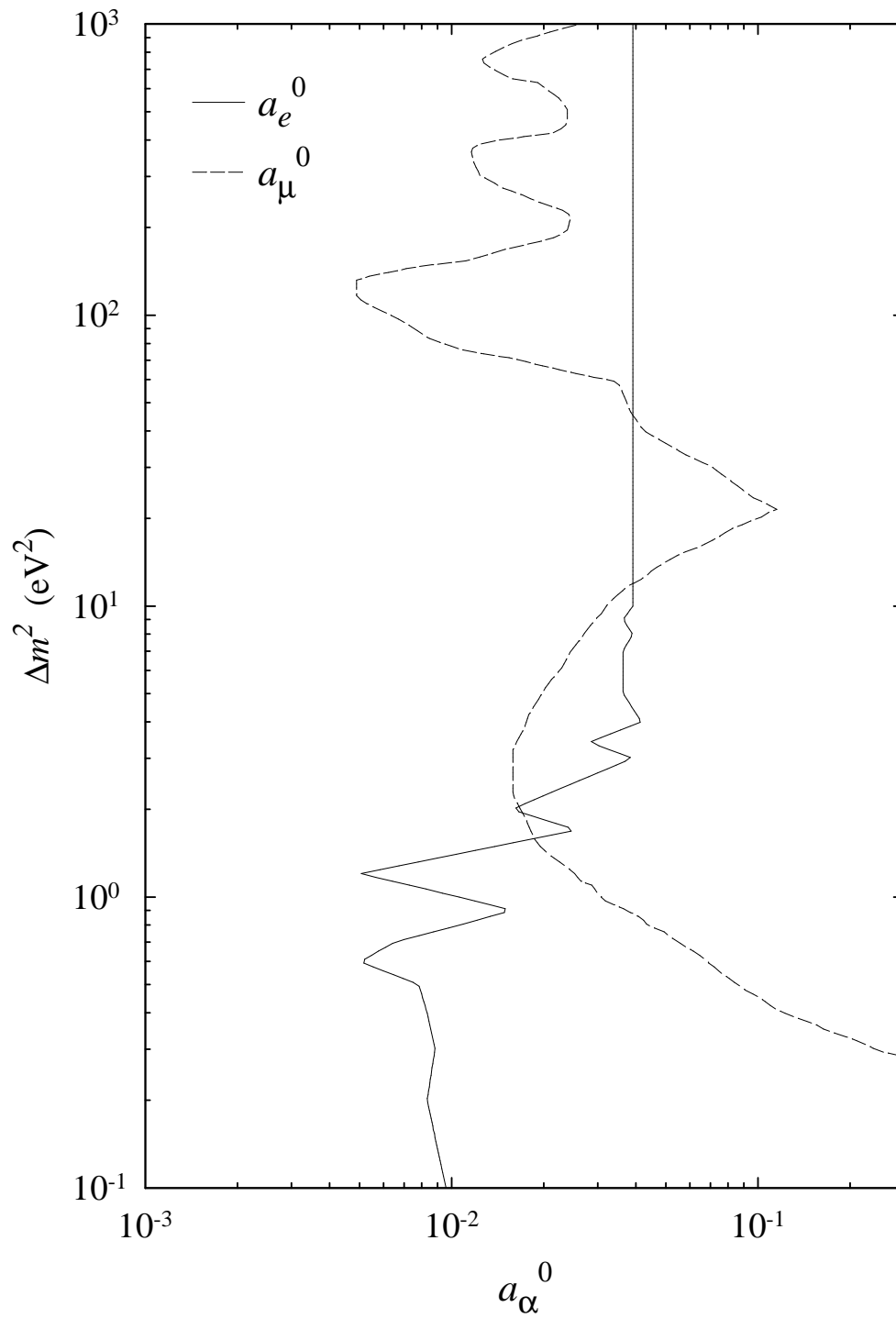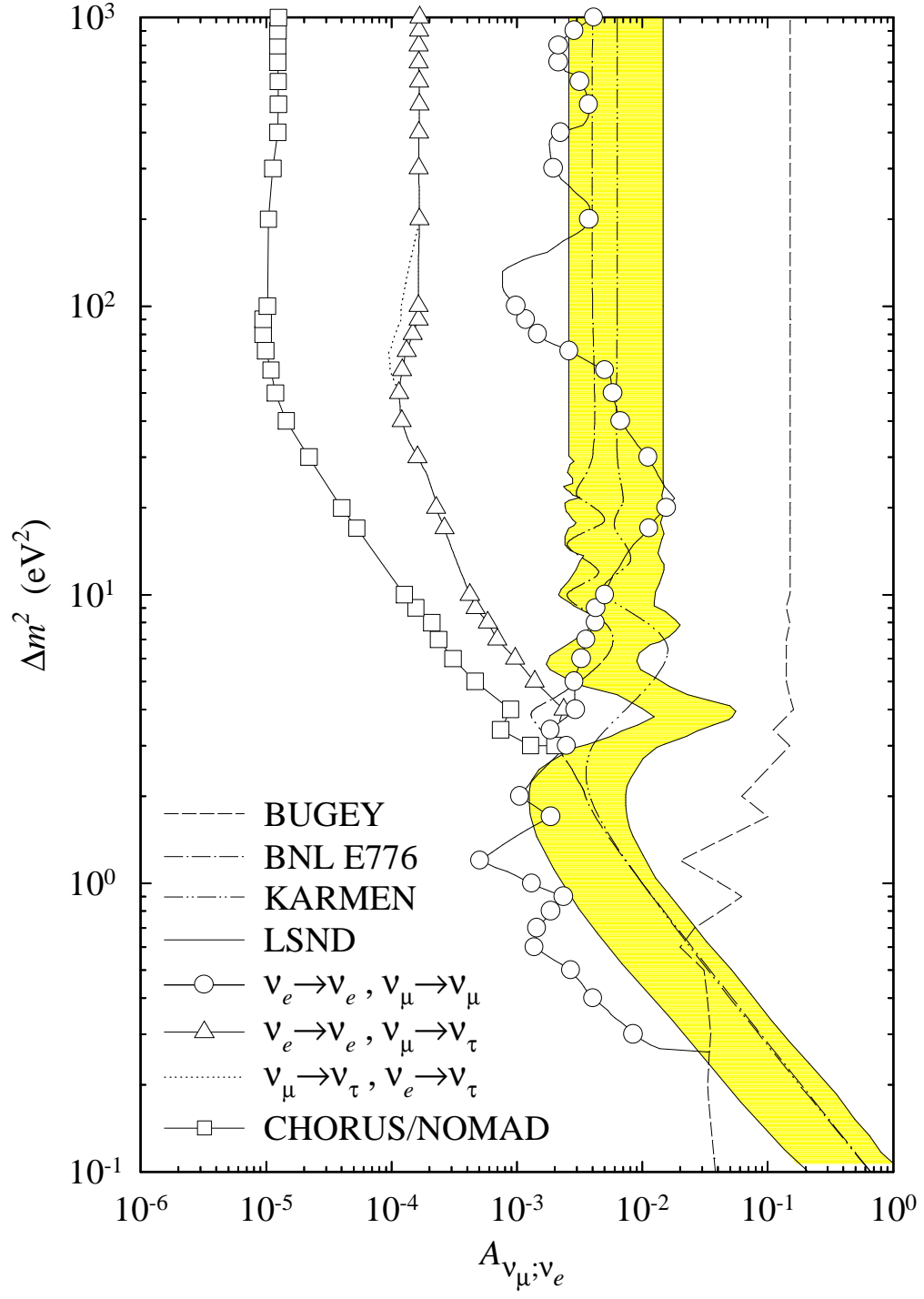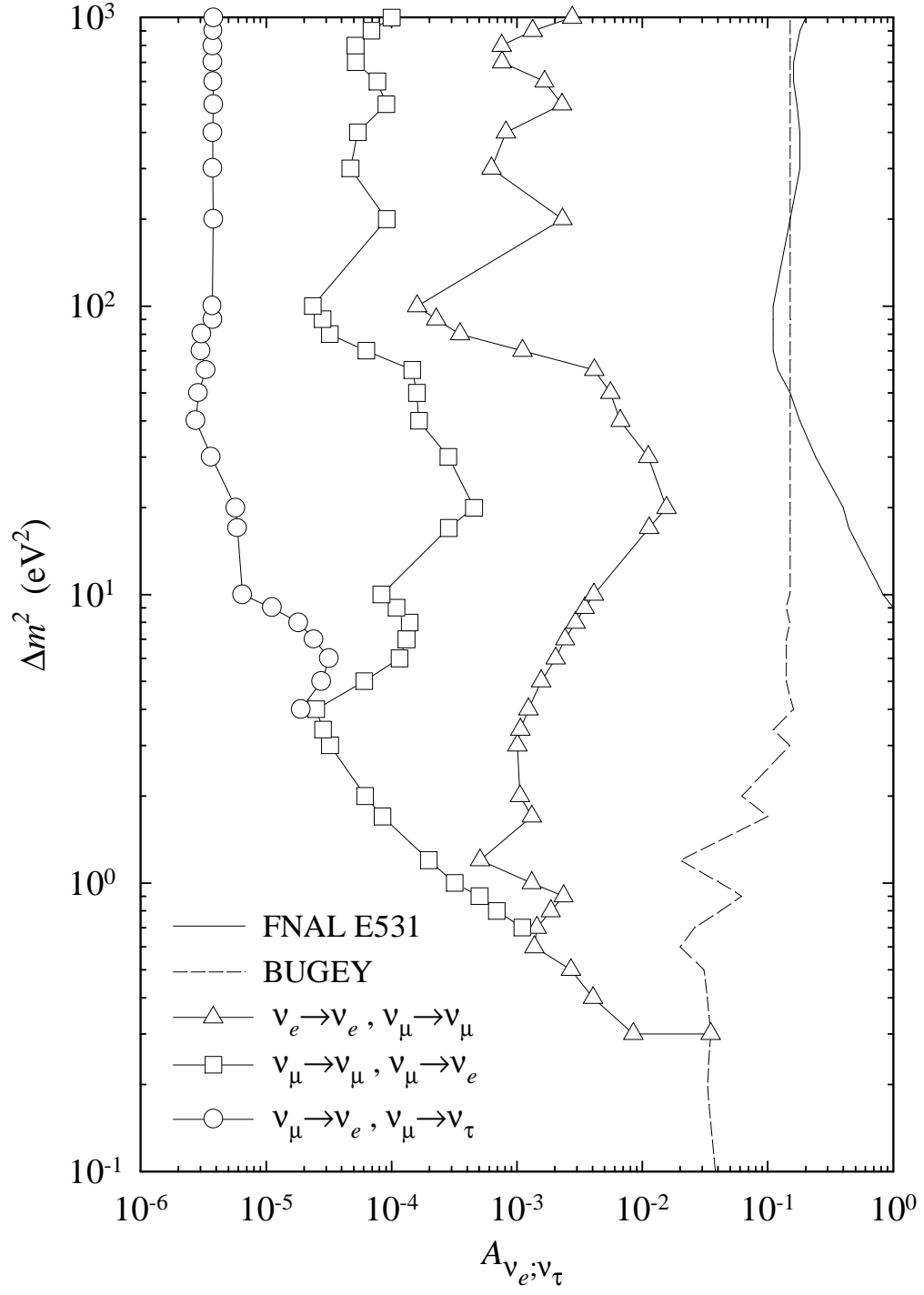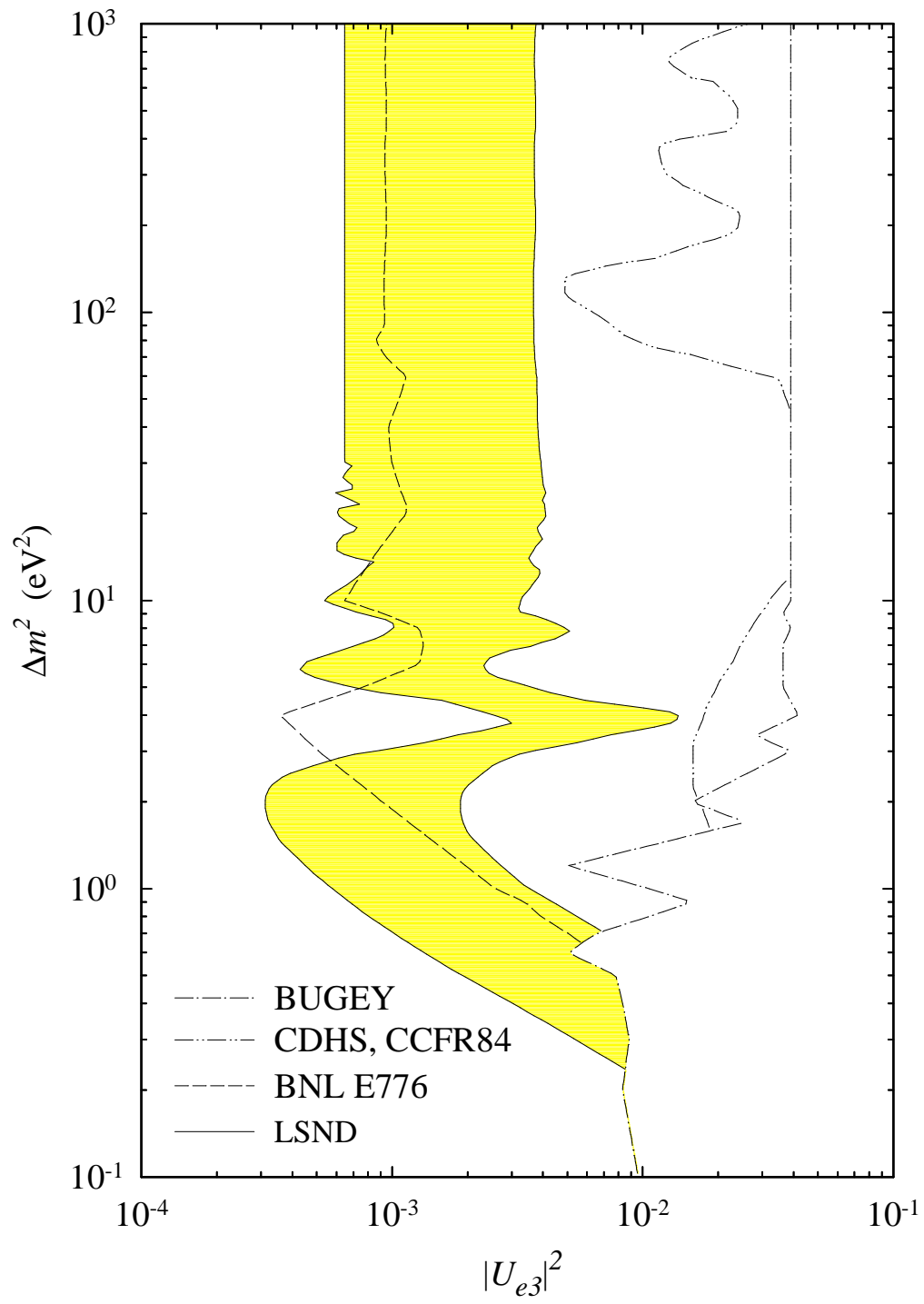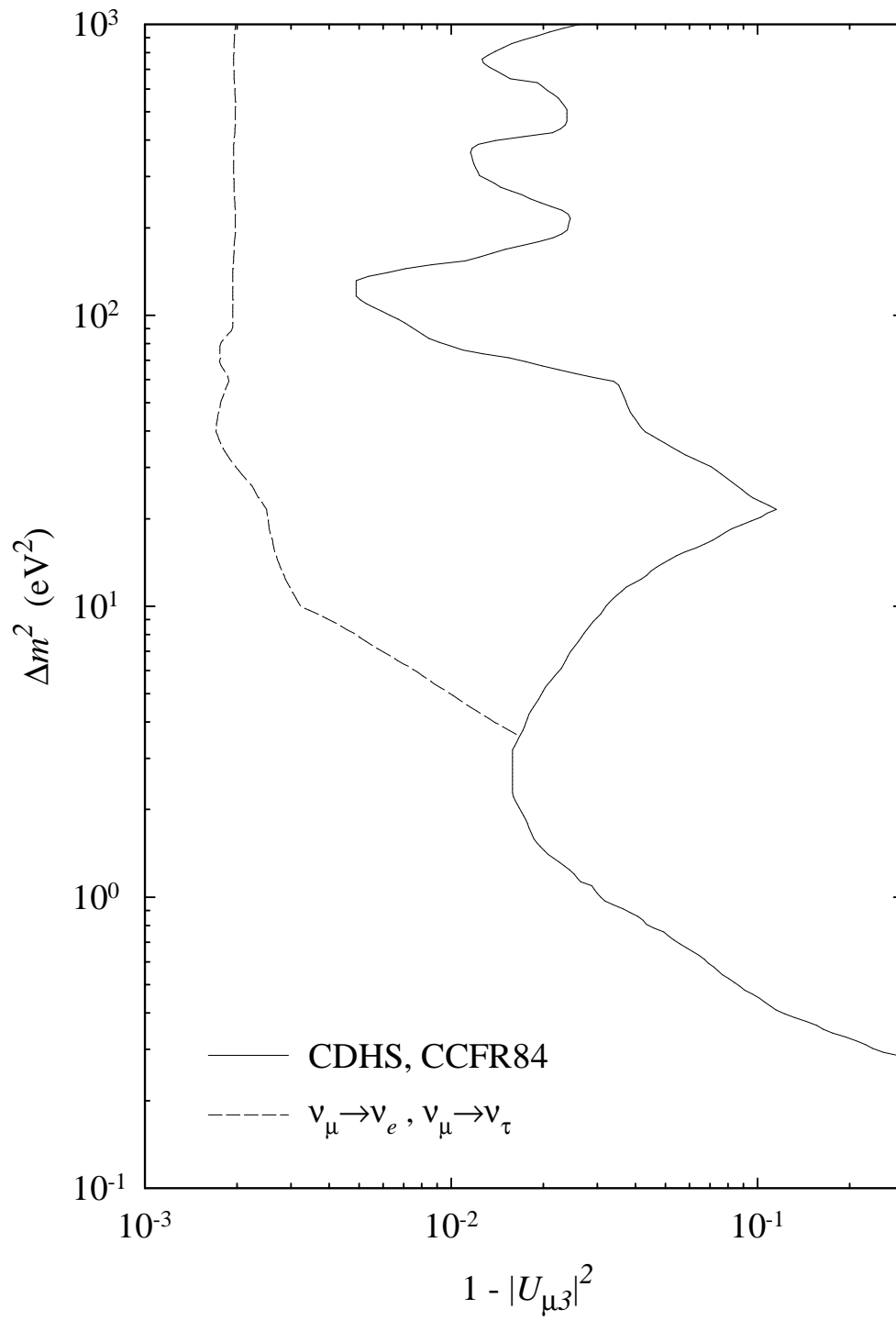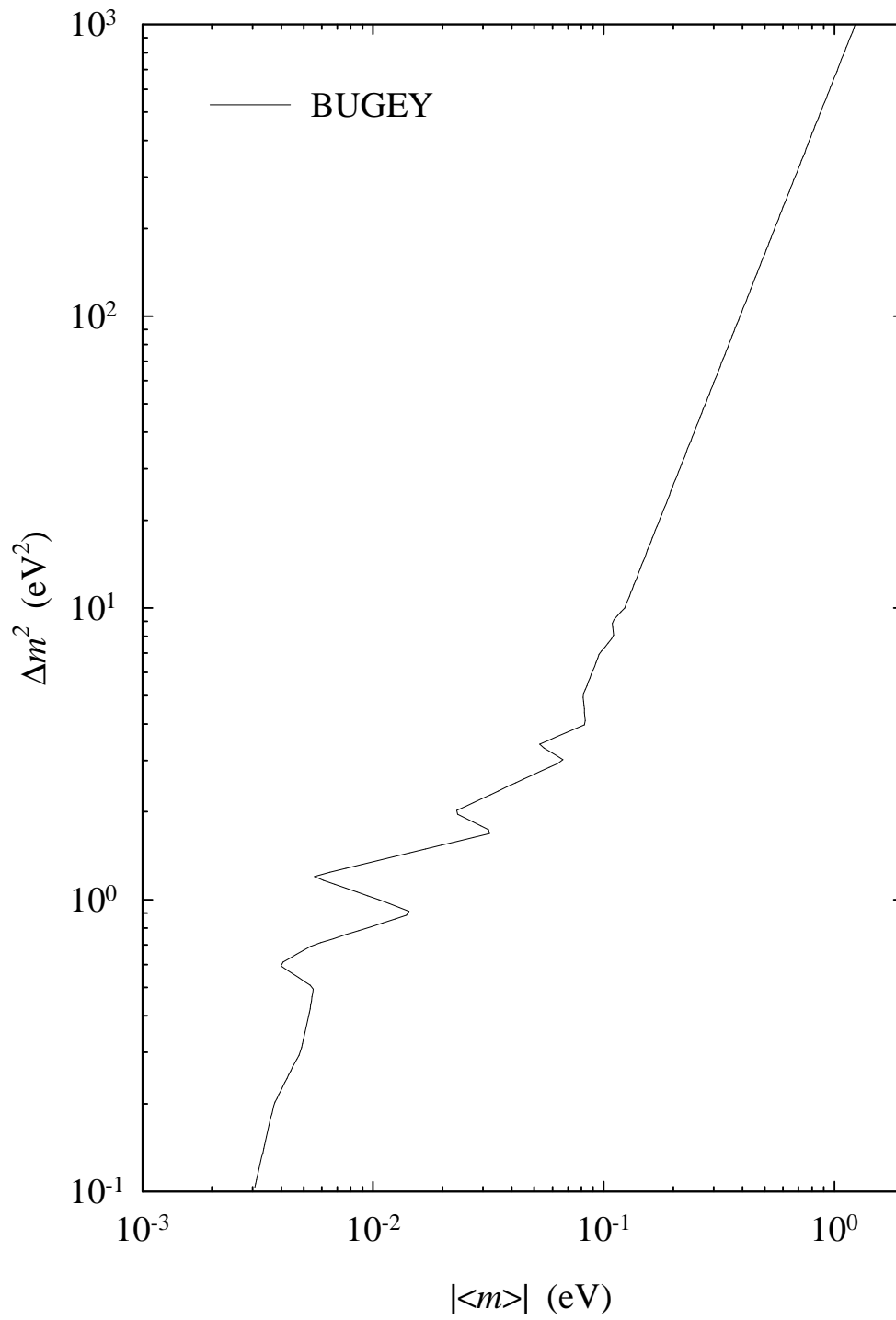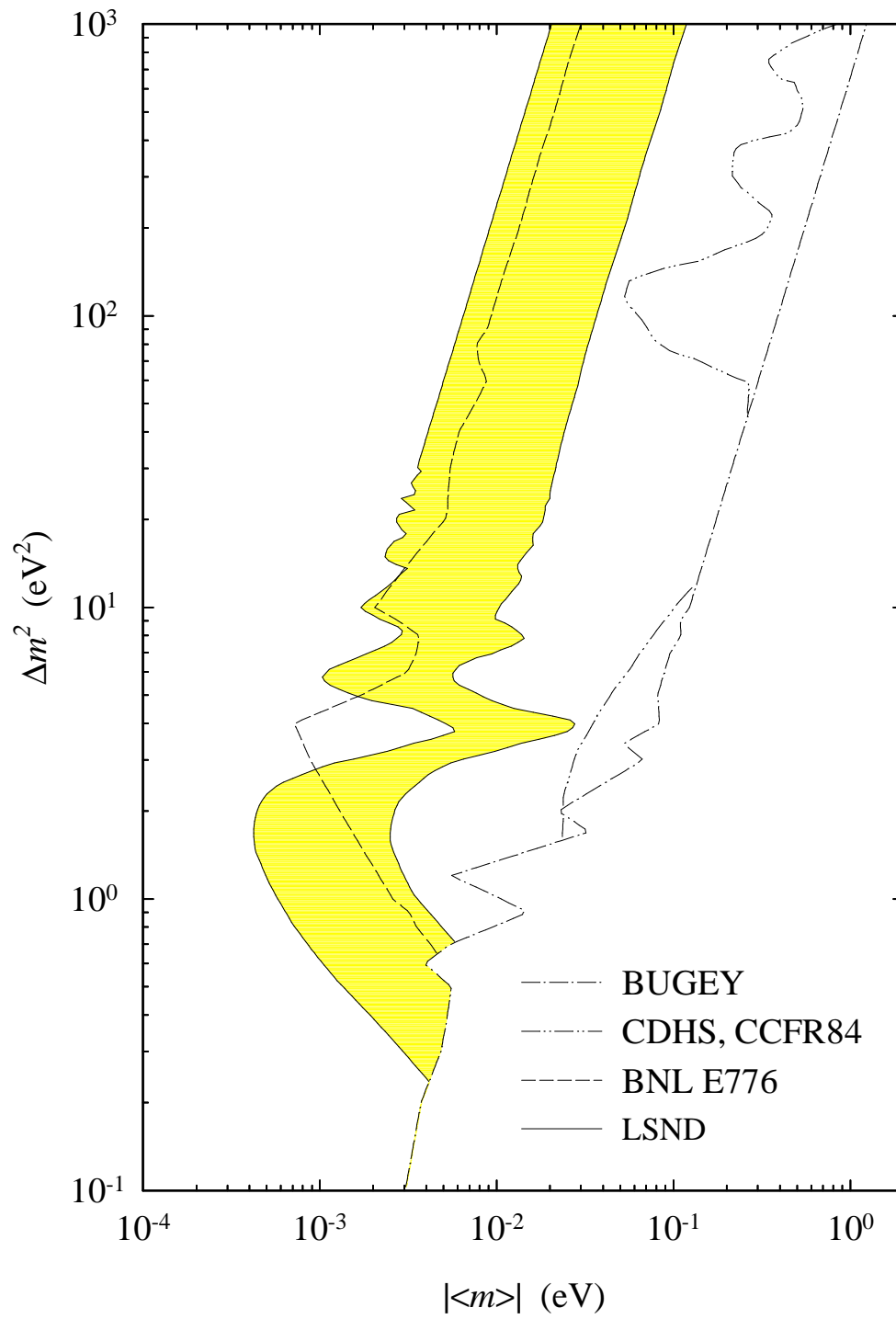
Figure 1

Figure 2

Figure 3

Figure 4

Figure 5

Figure 6

Figure 7

Figure 8

Figure 9